Research Article

Magnetic Fe$_3$O$_4$/MnO$_2$ core–shell nano-composite for removal of heavy metals from wastewater

Qiuju Li[1] · Fanxi Yang[2] · Jixin Zhang[3] · Cang Zhou[3]

Abstract

Feasible reutilization of sorbents was crucial to the waste water treatment process cost-effective and environmental friendly. Magnetic Fe$_3$O$_4$/MnO$_2$ composites as sorbents were recycle utilized to remove heavy metals ions [Pb(II), Cu(II), Cd(II) and Zn(II)] from industrial wastewater. In this paper, The Fe$_3$O$_4$/MnO$_2$ composites structure and interface adsorption mechanism were investigated by chemical affinity, Zero potentials combining with XRD, FTIR and TEM. The adsorption, desorption and recycle experiments were explored. The results indicated that Fe$_3$O$_4$/MnO$_2$ composites were nano structure with consisting of two layers with Fe$_3$O$_4$ in the core and amorphous MnO$_2$ on the shell. The adsorption mechanism was that the heavy metals substituting for H of Mn–O–H and forming the structure of Mn–O–Me which meant the metals removal was the process of ion exchange. The sorbent removal efficiency of Cu, Cd, Pb and Zn were 99.81%, 99.76%, 98.1%, 83.25%, respectively. The equilibrium data analysis indicated that the Langmuir model was the most appropriate model to describe the adsorption of on the surface of Fe$_3$O$_4$/MnO$_2$ composites. The kinetics studies showed that the adsorption kinetics of heavy metal ions on the surface of Fe$_3$O$_4$/MnO$_2$ composites was significantly appropriate to pseudo-second-order model. The experiments verified that the Fe$_3$O$_4$/MnO$_2$ sorbent being separated from water by external magnetic field for recycling was feasible for environmental friendly and efficient remove heavy metal ions.

Keywords Metallurgical wastewater · Magnetic Fe$_3$O$_4$/MnO$_2$ composites · Heavy metals removal · Surface adsorption mechanism · Recycle sorbent

1 Introduction

Contamination of soils and sediments with trace metals was worldwide problem originating from many industrial activities, such as ore processing, printing, metallurgy, batteries, electroplating, miningand chemical [1–4]. Heavy metal ions such as Pb, Cu, Cd and Zn were among the most common pollutants in industrial effluents [5–8], which did harm to human health and other living organisms. Consequently, Research had focused on the removal of metal ions contaminants to acceptable level of environmental friendly. In recent years, various methods for heavy metal removal from wastewater had been extensively studied. Various approaches, such as chemical precipitation, electrochemical treatment, ion exchange and adsorption, had been proposed to remove heavy metal ions from contaminated water [9–12]. Among these methods, adsorption was an attractive approach in contaminated water treatment, due to its high removal efficiency reliability, economy and without yielding harmful by-products [13].

Recently numerous approaches had been studied for the development of cheaper and more effective mineral adsorbents. Minerals had been increased attention for heavy metals remediation applications for high sorption

SN Applied Sciences
A SPRINGER NATURE journal

capabilities for metal [14–18]. Particularly, the nanostructure mineral offereinglarge surface areas, which provided high capacity and theability to enhance contaminant affinity with the surface [19, 20]. Therefore, MnO_2 had been chosen to prepare composited sorbents to adsorb heavy metals [21–25]. Unfortunately, such minerals still suffered from issues involving inconvenience of separation from the waste water as they tended to form super fine particles in aqueous solution and cause secondary pollution. Thus, the development of new nanosorbents with a facile separation property and recycling utilitywas of great interest. Iron oxide like magnetite (Fe_3O_4) and maghemite (γ-Fe_2O_3), had been extensively applied in designing because they had a high magnetic susceptibility. The modification of Fe_3O_4 with MnO_2 was not only removal heavy metal ions efficiently but also recovery through its magnetic property.

The adsorption was found to be accomplished by surface complexation. There was a lack of knowledge about the surface structure-sencentive adsorption and adsorption mechanism. How the parameter inpact on henvy metals adsorption, and the adsorbts worked efficiency after times recycle were still not clear. In this paper, the Fe_3O_4/ MnO_2 composites were used as cyclic sorbent to remove the heavy metals ions such as Pb(II), Cu(II), Cd(II) and Zn(II) from industrial wastewater. The surface structure and porpertiy of Fe_3O_4/MnO_2 composites were characterized. The influent parameters of remove heavy metals from waste water were investigated. Chemical affinity and total capacity of the composites were shown to be superior to select heavy metals in the wastewater. The surface adsorption isotherm and kinetics of Fe_3O_4/MnO_2 composites were investigated. The adsorption and desorption and the recycle remove of heavy metals were explored. The removal heavy metals mechanisms of Fe_3O_4/MnO_2 composites sorbent were elucidated.

2 Experimental sections

2.1 Synthesis of magneticFe$_3$O$_4$/MnO$_2$ composite

The magnetic composites Fe_3O_4/MnO_2 were prepared with a simple hydrothermal processon the basis of previous literature reports [26], and the modifications was needed in this experiment. During the synthesis process, 0.51 g $KMnO_4$ was first dissolved in 35 mL of deionized water. 0.8 mL HCl (37 wt%) was slowly added to the solution and stirred for 30 min.Then 0.32 g Fe_3O_4 was added into the solution and stirred continuous for 1 h. The mixture was washed with deionized water, and then dried at 120 °C for 2 h under atmospheric conditions.

2.2 Characterization of magnetic Fe$_3$O$_4$/MnO$_2$ composites

The morphologyof the products was examined by field-emission scanning electron microscopy (SEM) and transmission electron microscopy (TEM). Crystalline phases were identified by X-ray diffraction (XRD). Magnetic property measurement was performed on vibrating sample magnetometer (VSM). Surface area and pore size distribution were measured by the Brunauer–Emmett–Teller (BET). The zeta potentials were measured with a zetasizer. In order to obtain information about the distribution of metals ion within the Fe_3O_4/MnO_2 nano-composites, the samples were immerged with waste water for 24 h. The interaction between heavy metal ions and the adsorbent were examined by FTIR. The elemental compositions were determined by EDX and inductively coupled plasma atomic emission spectrometry (ICP). The pH_{PZC} (point of zero charge) of composites was defined as the pH value at which the surface carries net zero charge. To evaluate the pH_{PZC}, the acid and base titrations were carried out, and the corresponding pH was recorded using a pH meter.

2.3 Experiment of recycle remove heavy metals from waste water

Industrial waste water contained heavy metals (Zn, Pb, Cd, Cu) with the concentration of 10 mg L^{-1} of each metal. The magnetic Fe_3O_4/MnO_2 composite were applied as sorbent to remove heavy metals from industrial waste water. Fe_3O_4/MnO_2 composites sorbent was placed into the waste water and shaken for 24 h on a rolling mixer (20 rpm). The remove heavy metals experiments were performed at pH ranging from 2 to 12 and temperature ranging from 30 to 60 °C. The composites sorbent were then collected from the solution using a NdFeB magnet. The waste water (after remove the heavy metals) was analyzed by inductively coupled plasma atomic emission spectrometry (ICP). Each batch experiment was repeated thrice and the relative error was found to be within ± 2%, and the final data were the average values.

The removal degree was estimated by the capality of removal heavy metals in solution before and after adsorption, the formulas was shown as follow:

$$q_e = \frac{c_0 - c_e}{c_0} \times 100\% \tag{1}$$

where q_e (%) was removal degree, C_o and C_e (mg L^{-1}) were the initial and final metals concentrationsin the solution, respectively.

For the desorption experiment, Fe_3O_4/MnO_2 loading heavy metal ions was dipped into 0.1 M HCl solution, the mixture solution was stirred continuously in a shaker for 0.5 h at 30 °C. The composites sorbent were then collected wiht a NdFeB magnet and then concentrations of metal ions in the solution were analyzed. Fe_3O_4/MnO_2 composites was used in the next adsorption cycle after washing and drying. The quantity of ions desorption per unit mass of used adsorbent were calculated according to the following equations:

$$q_{de} = \frac{CV_0}{m_0} \times 100\% \tag{2}$$

While q_{de} (%) was desorption degree (%), C was the metal ion concentrations in the desorption solution (mg L^{-1}), V_0 is the volume of the desorption solution (L), m_0 was the heavy metal ions amount in before desorption (mg).

2.4 Adsorption isotherms

Langmuir and Freundlich models were the usual models for investigating the adsorption isotherms [27, 28]. Langmuir adsorption isotherm offered the homogeneous adsorption activation energy of adsorbent and envaluated the maximum adsorption capacity. Furthermore, this isotherm presumed monolayer adsorption. The linear form for the Langmuir isotherm model was expressed as Eq. (3). Freundlich isotherm described both monolayer and multilayer adsorptions. Freundlich isotherms were often used to describe adsorption equilibria between solid and solution. The linear form for the Freundlich isotherm model is expressed as Eq. (4):

$$\text{Langmuir equation:} \quad \frac{C_e}{q_e} = \frac{1}{kq_m} + \frac{C_e}{q_m} \tag{3}$$

$$\text{Freundlich equation:} \quad \log q_e = \log k' + \frac{1}{n} \log C_e \tag{4}$$

where the C_e and q_e were the equilibrium concentration of heavy metal ions (mol L^{-1}) and the amount of heavy metal ions adsorption on the mineral at equilibrium (mg g^{-1}), respectively. k was the Langmuir isotherm constant, and q_m was the maximum monolayer coverage capacities (mg g^{-1}), n was related to adsorption capacity and k' was the Freundlich isotherm constant (mg g^{-1}) (L mg^{-1}).

2.5 Adsorption kinetics

Study of the adsorption kinetics provided the rate of adsorbed heavy metal ions on the surface of sorbent.

Pseudo-first and pseudo second order models were the most common kinetic models used for modeling the kinetic rates [29].These models were also estimated the amount of adsorbed heavy metals on the surface of sorbent at various time intervals. The equations of these models can be expressed as follow.

The pseudo first order kinetic equation was represented by Eq. (5).

$$\ln(q_e - q_t) = \ln q_e - k_L t \tag{5}$$

The pseudo second order (PSO) kinetic equation was represented by Eq. (6).

$$\frac{t}{q_t} = \frac{1}{kq_e^2} + \frac{1}{q_e}t \tag{6}$$

where q_e and q_t was the heavy ions adsorption quantity (mg g^{-1}) at equilibrium time and time t, respectively, k_L and k were the rate constants of pseudo-first and second order models, respectively. q_t had exponential relation with t in the pseudo-first-order model while the relation between t/q_t and t was linear for the pseudo-second-order model.

3 Results and discussion

3.1 Characterization of Fe_3O_4/MnO_2 composite

A series of characterization methods were used to characterize Fe_3O_4/MnO_2 composite. The phase structure of composites particles were characterized with XRD showed in Fig. 1. The patterns of Fe_3O_4/MnO_2 composites were similar with that of Fe_3O_4, but the peaks strength of Fe_3O_4/MnO_2 composites were weaker compared with that of Fe_3O_4. In addition, all the diffraction peaks were identified to
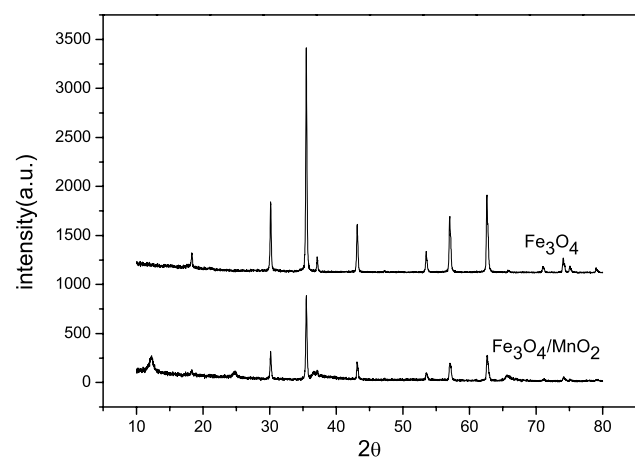
Fig. 1 XRD patterns of Fe_3O_4 and Fe_3O_4/MnO_2 composites

face-centered cubic crystal of Fe_3O_4 (space group: Fd3m, a = b = c = 8.394 A). No visible MnO_2 crystalline peaks were detected in all lines, which inferred that out shell MnO_2 was amorphous phase.

Figure 2 displayed TEM images of Fe_3O_4/MnO_2 composites. The TEM image in Fig. 2a gave an overview of the sample, these particles with uniform spherical shape and loosely arranged with the average size 90–100 nm. Figure 2b presented the aggregation of small particles and an amorphous light grey shell covered on the dark core could be clearly identified. It was showed that the core with 50 nm size was covered with out shell of 40–50 nm thickness. The main elements of the core were Fe and O menat Fe_3O_4, and the shells contained Mn and O which meant the amorphous shell was coated with MnO_2 according to the energy dispersive spectrum (EDS) analysis. MnO_2 content in core–shell structure Fe_3O_4/MnO_2 nano-composites was about 18wt % calculated through ICP-AES analysis. The core–shell structure of Fe_3O_4/MnO_2 nano-composites was confirmed by the IR spectra analysis.

Infrared spectrum was operated to analysis the spectrums of the sorbent Fe_3O_4/MnO_2 nano-composites, ferroferric oxide and manganese dioxide. The infrared scanning range was 400–4000 cm^{-1}. Referred to the standard infrared spectrum of ferroferric oxide and manganese dioxide, the absorption peaks at 584 cm^{-1} was the Fe–O characteristic absorption peak and peak at 3400 cm^{-1} was stretching vibration of hydroxy ferric iron. The infrared absorption peaks at 3400 cm^{-1}, 1625 cm^{-1}, 1348 cm^{-1}, 553 cm^{-1} were infrared characteristic peaks of manganese dioxide. And the peak at 3400 cm^{-1} was the surface hydroxyl stretching vibration peak of Mn–O, the peak at 1625 cm^{-1} was the stretching vibration peak of the combination of Mn–O and O–H. As shown in Fig. 3, the absorption peaks of Fe_3O_4/MnO_2 composites happened at the characteristic

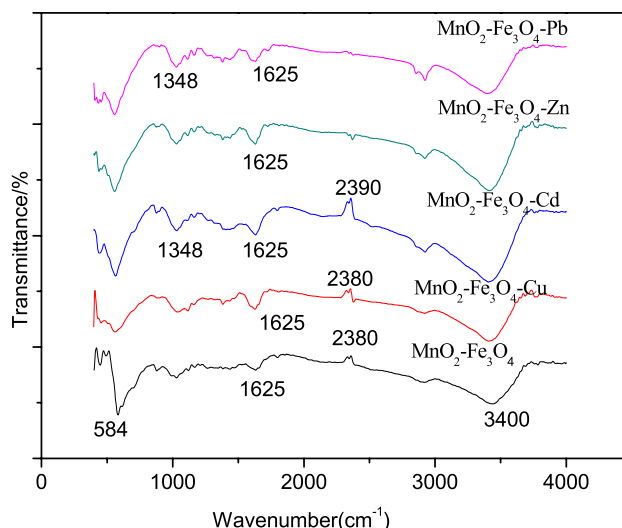**Fig. 3** FTIR spectrums for Fe_3O_4/MnO_2 adsorption heavy metals

absorption peaks of ferroferricoxide and manganese dioxide, which proved that this nano-composites sorbent was a composite product of Fe_3O_4 and MnO_2.

Zeta potential measurements were conducted to understand the electrostatic interactions between the surfaces and the aqueous species, and Fe_3O_4/MnO_2 composites and Fe_3O_4 powder were positively charged. The result of zeta potential measurements agreed well with surface charges expected from the reported pH_{PZC} values of these minerals. The pH_{PZC} value for Fe_3O_4 was 6.2 and the pH_{PZC} value for Fe_3O_4/MnO_2 nano-composites was 3.25 much lower than that of Fe_3O_4 powder. The results indicated that the composite could facilitate to adsorb more positively charged heavy metal ions in a wide range of pH values. BET were used to determine the surface area of and

Fig. 2 TEM images of Fe_3O_4/MnO_2 composites
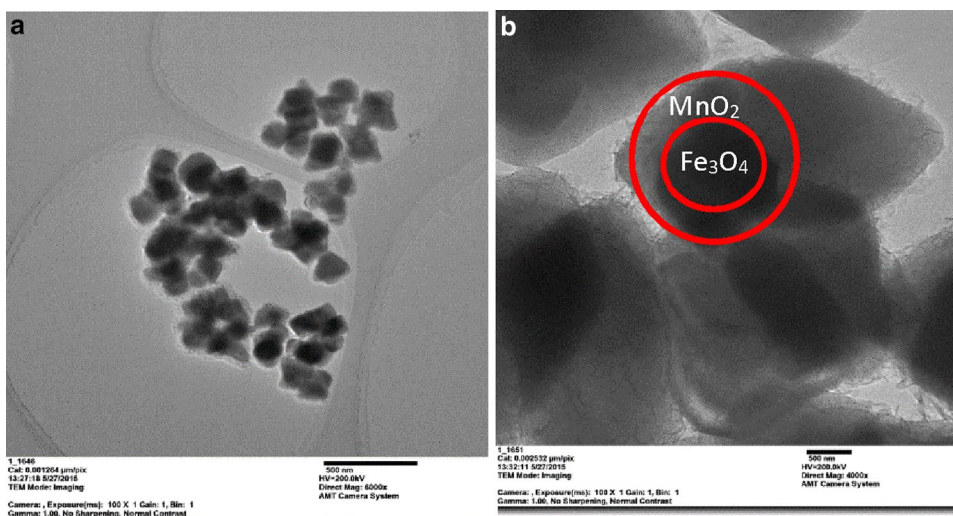
the surface area s was 69.23 $m^2 g^{-1}$, which meant Fe_3O_4/MnO_2 nano-composites with high specific surface area and high adsorption ability.

3.2 Surface adsorption structure studies

The FTIR analysis of Fe_3O_4/MnO_2–Me (Fe_3O_4/MnO_2 adsorbed Cu, Cd, Zn, Pb) were showed in the Fig. 3. The infrared absorption peaks 3400 cm^{-1} was the surface hydroxyl stretching vibration peak of manganese dioxide, the peak at 2380 cm^{-1} was the stretching vibration peak of the combination of manganese atoms and O–H. Mn–OH infrared peak depth at 1625 cm^{-1} changed with adsorption of different heavy metal ions. The depth of absorption peak of cadmium ion was clearly greater than that of copper, zinc and lead ion. The adsorption sequence was Cd > Cu > Zn > Pb, which related with before adsorption capacity andtheir affinity with the adsorbent. The change of Mn–OH infrared adsorption peak incidicated heavy metal ions would institute H ion as adsorbingmetals ions, andformed the structure of O–Me (Me meant Cu, Cd, Zn, Pb) on the surface of sorption. The infrared absorption peak at 2890 cm^{-1} was simple surface electrostatic exchange. The Fe–O absorption peak at 584 cm^{-1} obviously changed, which not only proved that the adsorption of heavy metal ions happened on manganese dioxide, the ferroferricoxide was also involved in the adsorption simultaneously.

The FTIR analysis also showed Fe_3O_4/MnO_2 structures which adsorption heavy ions under different ions content waste water. The Mn–O–H absorption peak at 2380 cm^{-1} obviously changed, and the intensity increased with adsorption Cd and Cu which meant Mn–O–H structure broken and Mn–O–Cd and Mn–O–Cu formed. The results showed that the vibrational band of Mn–OH fell off at and 1348 cm^{-1} and 1625 cm^{-1} with the metals contents in wastewater increasing. That reason was that the metals content increased and enriched at the surface of absorption, and the heavy metals substituted for H of Mn–O–H and formed the structure of Mn–O–Cu, Mn–O–Cd, Mn–O–Zn and Mn–O–Pb which meant the metals remove was the process of ion exchange.

The surfaces of the metal oxides (MnO_2 suspension) were generally covered with hydroxyl groups that vary with their form at different pH. The isoelectric point (IEP) of Fe_3O_4/MnO_2 nano-composites was found to be around pH 3.25. At low the value of pH, there were much H^+ on the surface of Fe_3O_4/MnO_2 nano-composites sorbent which was not good for heavy metals removal. The heavy metal ions such as Cu^{2+}, Cd^{2+}, Zn^{2+}, Pb^{2+} had strong possibility of polarity in the weak acidic waste water, and formed the structure of $Cu(H_2O)_6^{2+}$, $Cd(H_2O)_6^{2+}$, $Zn(H_2O)_6^{2+}$, $Pb(H_2O)_6^{2+}$. When the pH value

was between 4.0 and 6.5, there was a declining H^+ on the surface of Fe_3O_4/MnO_2 nano-composites sorbent.

It was shown positive potentialwith the pH value higher than 6 after adsorption of Cd^{2+}(Cd^{2+} was chosed as model adsorbate). The result showed that the manganese dioxide played a decisive role in sorbent, and the main principle of adsorption was the positive charge exchange. Before adsorption of heavy metals ion, manganese dioxide maintained a certain amount of ionization balance in water, such as expression (7) and (8).

$$\equiv MnOH + H^+ \leftrightarrow \equiv MnOH_2^+ \qquad (7)$$

$$\equiv MnOH \leftrightarrow \equiv MnO^- + H^+ \qquad (8)$$
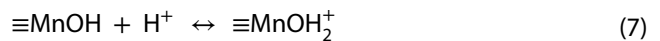
The adsorption of heavy metals ion, positive charge exchange took place between heavy metalsion and manganese dioxide with high pH in waste water, such as expression (9) and (10), where Me was representational for heavy metals of Cu, Cd, Pb and Zn. The heavy metals ion replaced more hydrogen ions, so the zeta potential of the solutionin the direction of the alkaline, at the same time, this phenomenon also proved the mechanism of the cadmium ions adsorption waspositive charge exchange.

$$\equiv MnOH + Me^{2+} \leftrightarrow \equiv MnOMe^+ + H^+ \qquad (9)$$

$$\equiv 2MnOH + Me^{2+} \leftrightarrow \equiv (MnO)_2Me + 2H^+ \qquad (10)$$
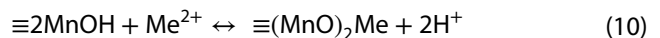
The sorbent of Fe_3O_4/MnO_2 nano-composites was the shell core structure with MnO_2 amorphous shells and ferromagnetic cores which enhanced its ability of sorption analyzied by FIIR and zeta potentials and became attractive for absorption materials. The sorbent of Fe_3O_4/MnO_2nano-composites adsorbing heavy metals was enriched with magnet and dried at 200 °C for several days. The sorbent was analyzied by XRD indicates that heavy metals such as Cu, Cd, Zn and Pb substitution H precipitated in MnO_2 and Me–O–Mn mineral recrystallization formed. So the adsorption site was on MnO_2 surface and Fe_3O_4 was just a basic carrier.

3.3 Adsorption studies

The degrees of remove heavy metals of Fe_3O_4/MnO_2 nano-composites were shown in Fig. 4. The results showed that Fe_3O_4/MnO_2 nano-composites had relatively high adsorption capacity owing to their larger surface area, which contributed to the increase in the number of adsorption sites for the heavy metals. In addition, MnO_2 had abundant surface functional groups
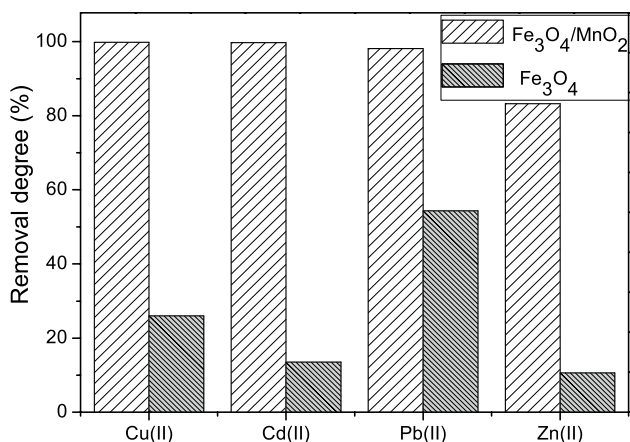
Fig. 4 Adorption of Pb, Cu, Znand Cd on Fe$_3$O$_4$/MnO$_2$nano-composites and Fe$_3$O$_4$ (Me: 10 mg L^{-1}, [sorbent]:1 g L^{-1}; pH 6.5; time: 24 h)

and high-density negative charges verified before. The removal degrees of the four heavy metal ions Cu, Cd, Pb and Zn were 99.81%, 99.76%, 98.1% and 83.25% respectively.

The dosage of sorpent for removal heavy metals from waste water was significant for efficiency. The effect of dosage on Fe$_3$O$_4$/MnO$_2$ nano-composites remove heavy metals was shown in Fig. 5. The removal of heavy metals from waste water increased obviously with the increase of Fe$_3$O$_4$/MnO$_2$ nano-composites dosage when the dosage was less than 1.0 g L^{-1}. As the Fe$_3$O$_4$/MnO$_2$ nano-composites dosage increased, the number of available sites for binding heavy metal ions increased, which could improve the removal heavy metal ions. When the dosage of Fe$_3$O$_4$/MnO$_2$ nano-composites increased to excass 1.0 g L^{-1}, the
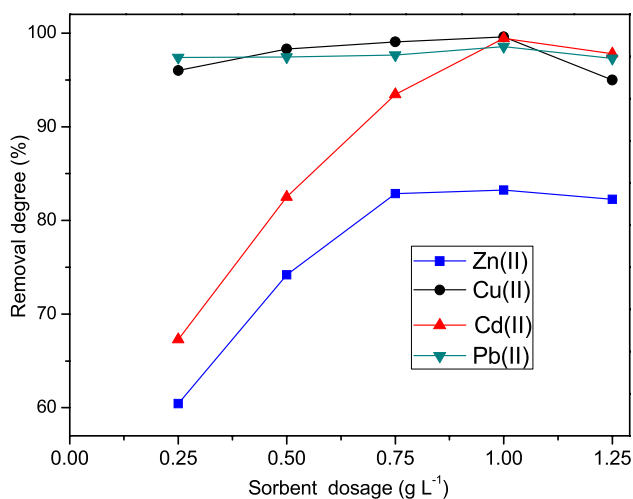
mounts of removal heavy metals decreased. The result was that the increase of sorbent dosage could decrease the contact area between metal ions and solid surface.

pH effect on Fe$_3$O$_4$/MnO$_2$ nano-composites adsorption Cu, Cd, Pb and Zn were conducted at atmosphere temperature as showed in Fig. 6. These heavy metals removal degree were increased with of pH increasing to 6.5 and then arrived at a maximum removal with pH exceed 6.5. The maximum adsorption dehree of Cu, Cd and Pb was almost 99%, and the maximum adsorption dehree of Zn was 88%. The results showed Fe$_3$O$_4$/MnO$_2$ nano-composites removed these heavy metals in waste water with high pH, which meant pH affected the sorbent surface charge distribution and surface species adsorption. The adsorption capacity were found to be increased with the pH increasing. Cd and Zn were hardly adsorbed, and the removal degree of Cu, Pb were relatively low with pH lower than 4.0, because the adsorbent surface would acquire a positive charge when pH was less than 3.25 (pH$_{pzc}$) [30]. As pH > 4.0, hydrogen ion concentration in the solution decreased gradually, which could lead to the H$^+$ leaving Fe$_3$O$_4$/MnO$_2$ nano-composites surface. There was more negatively charged sites in the sorbent surface which was available to the metal ions and caused the adsorption capacity increased dramatically. When pH > 6.0, Fe$_3$O$_4$/MnO$_2$ nano-composites surface was nagetive electronegativity which was easy to adsorption positively charged metal ions according to the zeta potential measurements.

Heavy metals ions would be present in the species of Me^{2+}, Me(OH)$^+$, and Me(OH)$_2$ (Me: Cu^{2+}, Cd^{2+}, Zn^{2+} or Pb^{2+}) at different pH values in the aqueous solution. M^{2+} was the dominant specie at low pH, and it might be hydrolyzed to form Me(OH)$^+$ and M(OH)$_2$ with the pH increasing.
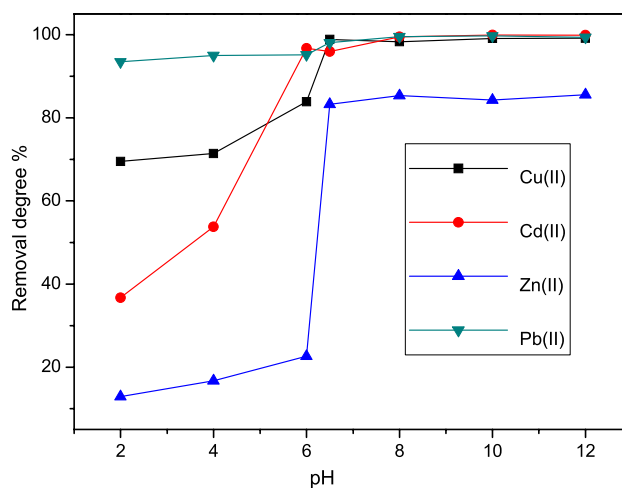

Fig. 5 Effect of Fe$_3$O$_4$/MnO$_2$ nano-composites dosage on Me adsorption (pH 6.5, initial Me concentration = 10.0 mg L^{-1})

Fig. 6 Effect of pH on Fe$_3$O$_4$/MnO$_2$ nano-composites adsorption of Me (Me: Cu, Zn, Pb and Cd) on (Dose: 1 g L^{-1}, Me 10 mg L^{-1}, time: 24 h)

The precipitation constants of $Pb(OH)_2$, $Cu(OH)_2$, $Zn(OH)_2$ and $Cd(OH)_2$ were 1.2×10^{-15}, 2.2×10^{-20}, 1.2×10^{-17} and 5.27×10^{-15}, and the precipitation played a main role when $pH > 9.7$, $pH > 7.4$, $pH > 8.0$ and $pH > 11$ with corresponding to metal ions concentration, respectively. Therefore, the most feasible pH value was selected as 6.5 for Cu, Cd, Zn and Pb removal which there were no hydroxide precipitations formed and the adsorption capacities were high enough.

The adsorption degree increased with temperature improving as showen in Fig. 7. Temperature effect on Cu, Cd, Zn or Pb removal were conducted at different temperature of 30 °C, 40 °C, 50 °C and 60 °C. The dosage was 1 g L^{-1}, and the inial heavy ion contents of 10 mg L^{-1}, adsorption of 24 h. The results showed that the adsorption of Zn was the most impacted by temperature. Zn
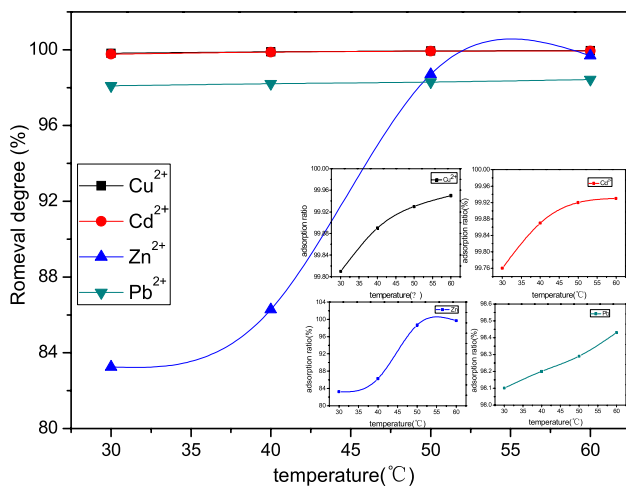
adsorption degree was 83.25% at 30 °C, and increased to 99.69% at 60 °C, while the adsorption degree of Cu, Cd, Pb arrived at 98% with the temerarture of 30 °C. Core–shell Fe_3O_4/MnO_2 adsorption zinc ions improved with temperature increasing meant which was an endothermic process. The Core–shell structure Fe_3O_4/MnO_2 adsorption heavy ions process were all endothermic which meant chemical adsorptions mechanism.

3.4 Adsorption isotherms

Adsorption isotherms were used to achieve more information about the adsorption behavior and adsorption parameters such as the adsorption maximum capacity on the surface of Fe_3O_4/MnO_2. The results of equilibrium data for Cu^{2+}, Cd^{2+}, Zn^{2+}, Pb^{2+} sorption were presented for Langmuir and Freundlich isotherm in Fig. 8a, b, respectively. As seen from Fig. 8a, the adsorption densities of heavy metal ions for sorbent were improved with increasing the concentration of metal ions, which confirmed that the initial concentration was a driven force for adsorption process.

The results of the two isotherm models as a function of heavy ions concentration at a pH of 6.5 and room temperature were presented in Table 1. The results showed that R^2 values of the Langmuir isotherm model was the higher than that of Freundlich isotherm model. Langmuir isotherm model was the best describing model for Cu^{2+}, Cd^{2+}, Zn^{2+} and Pb^{2+} adsorption on Fe_3O_4/MnO_2 surface. This model postulates that the monolayer adsorption of metal ions on the Fe_3O_4/MnO_2 surface with all adsorption sites would be formed and being energetically equivalent. All relations between C_e/q_e and C_e of heavy metal ionswere linear. The correlation coefficient value (R^2) except Cd^{2+} were higher than 0.99. As shown from
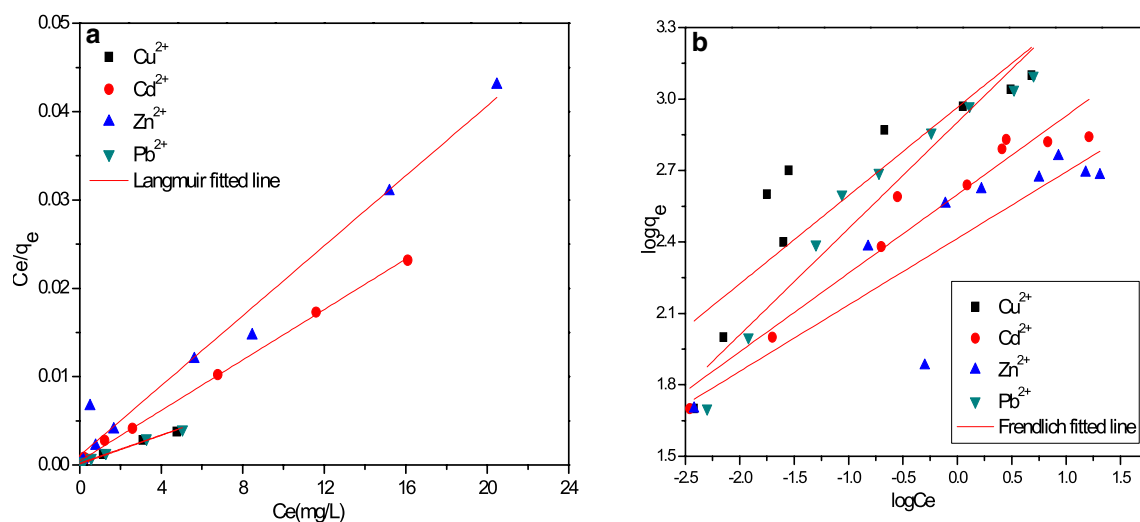

Fig. 7 Temperature effect on heavy metal ions adsorption

Fig. 8 **a** Langmuir isotherm for adsorption, **b** Freundlich isotherm for adsorption

Table 1 Comparison different parameters for various isotherm models

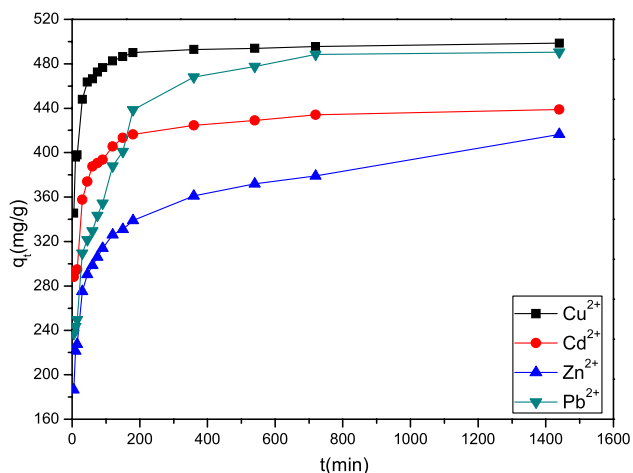| Metal ions	Langmuir isotherms			Freundlich isotherms		
	q_m (mg g^{-1})	k	R^2	k'	n	R^2
Cu^{2+}	498.575	7.94	0.9920	18.476	2.676	0.7902
Cd^{2+}	439	0.904	0.9708	8.033	2.930	0.9378
Zn^{2+}	416.5	1.88	0.9903	5.19	3.58	0.7299
Pb^{2+}	490.5	3.79	0.9917	15.94	2.24	0.9326

Fig. 9 Adsorption capacity of heavy metal ions varies with time

Table 1, the Maximum adsorption capacity q_m value of the Langmuir isotherm model for Fe$_3$O$_4$/MnO$_2$ adsorption Cu^{2+}, Cd^{2+}, Zn^{2+}, Pb^{2+} was 498, 439, 416.5 and 490 mg g^{-1}, respectively which was much higher than the references [31], which meant MnO$_2$ acted on the adsorption. The metal ions order according to Langmuir model were Cu^{2+} > Pb^{2+} > Zn^{2+} > Cd^{2+} according to the k values.

3.5 Adsorption kinetic

Figure 9 was the Fe$_3$O$_4$/MnO$_2$ adsorption heavy ions capacity change with time. The dosage was 1 g L^{-1}, with the inial heavy ion contents of 10 mg L^{-1}, and the temperature of 30 °C. The adsorption capacity q_t of Cu^{2+}, Pb^{2+}, Zn^{2+}, Cd^{2+} in waste water increased to 480 mg g^{-1}, 350 mg g^{-1}, 300 mg g^{-1} and 380 mg g^{-1} within 100 min. From the slope of the curve, it could deduce that the adsorption rate increased in 100 min, and then slow down during 100–200 min because of adsorption site reducing rapidly.

Figure 10a, b showed the kinetic adsorption parameters which were fitted by pseudo-first and pseudo-second-order models. A relatively higher correlation coefficient R^2 values of pseudo-second-order model was the higher than that of pseudo-first model. The pseudo-second-order models described well the adsorption kinetics of heavy metal ions on the surface of Fe$_3$O$_4$/MnO$_2$, which meant that the rate of adsorption should be proportional to the concentration of metal ions in the solution. Also, the rate of the adsorption was controlled by the chemical the exchange. These results revealed that the surface chemistry of minerals could be changed by surface dissolution.

The kinetic parameters of metal ions sorption process on composite were listed in Table 2. It was concluded that
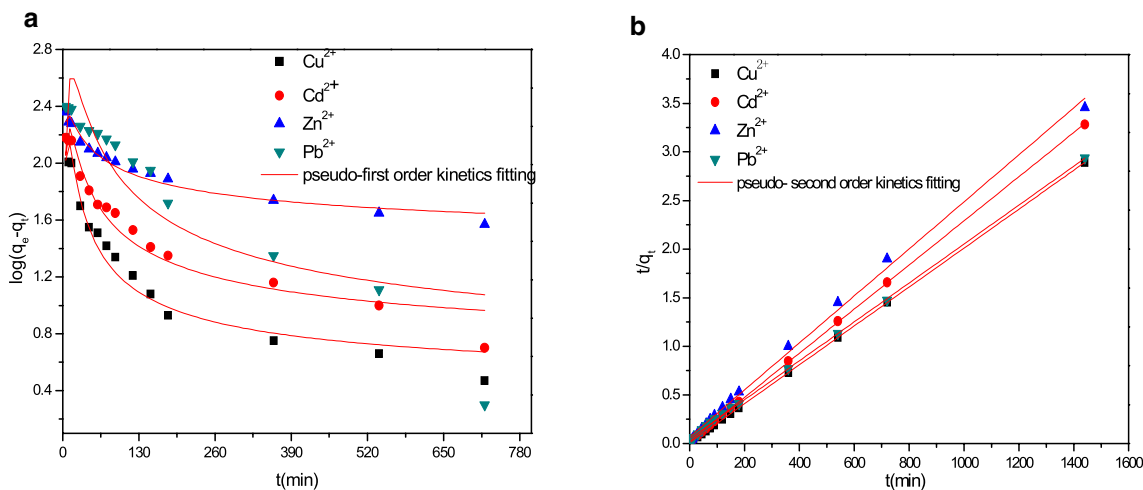
Fig. 10 **a** The pseudo-first order kinetics fitting, **b** the pseudo-second order kinetics fitting

Table 2 Kinetic adsorption parameters of Cu^{2+}, Cd^{2+}, Zn^{2+}, Pb^{2+}

Metal ions	Pseudo-first order		Pseudo-second order	
	K_L	R^2	K	R^2
Cu^{2+}	0.0053	0.9499	0.0286	0.9999
Cd^{2+}	0.0048	0.9403	0.0143	0.9999
Zn^{2+}	0.0025	0.9585	0.0049	0.9969
Pb^{2+}	0.0064	0.73896	0.0046	0.9994

the best fit of the experimental data was exhibited by the second order model for Pb^{2+}, Cd^{2+}, Zn^{2+}, Cu^{2+} sorption in which the determination coefficient (R^2) was higher than 0.99 and the values predicted from the experimental data q_e. The second order model for ions sorption with the rate constants k was equal to 0.0286 mg g^{-1} min^{-1} for Cu^{2+}, 0.0143 for Cd^{2+}, 0.0049 for Zn^{2+} and 0.0049 for Pb^{2+}, respectively. The low values of rate constant (k) suggested that the adsorption rate decreased with the increase of the phase contact time and the adsorption rate was proportional to the number of unoccupied sites. These results confirmed the mechanism of chemical adsorption involving valence forces through sharing or exchange of electrons between adsorbent, which was in good agreement with studies of literature based on MnO_2 [24].

3.6 Recycle of Fe_3O_4/MnO_2 nano-composites

For the desorption experiments, HCl was used to desorption metal ions from Fe_3O_4/MnO_2 sorbent loading heavy metal ions for 24 h, and the concentration of HCl was 0.1 M at temperature of 30 °C. Figure 11 showed the metal ions desorption reaction degree with 0.1 M HCl, and the desorption degree of Cu^{2+}, Cd^{2+}, Pb^{2+} and Zn^{2+} from Fe_3O_4/MnO_2 were increased at the first 25 min, while desorption degree of Pb increased at the first 50 min. The desorption degree of Cu^{2+}, Cd^{2+}, Pb^{2+} and Zn^{2+} from Fe_3O_4/MnO_2 nano-composites was to achieve the desorption equilibrium with 60 min later under our experimental condition. The desorption process was H$^+$ ion adsorption competing to that of heavy metal ions at adsorption sites.

Fe_3O_4/MnO_2 composites exhibited a poor adsorption capacity at lower pH, which acid treatment was likely to be a suitable approach for regeneration of sorbent Fe_3O_4/MnO_2 composites. Desorption process of Fe_3O_4/MnO_2–Me carrier was executed in the 0.1 M HCl solution with an ion-exchange mechanism. The dominant protonation between H$^+$ ions and metal ions on the active sites explained the desorption of metal ions from Fe_3O_4/MnO_2–Me. The structure of complexation Fe_3O_4/MnO_2 nano-composites with Cu^{2+}, Cd^{2+}, Pb^{2+} and Zn^{2+} were broken by H$^+$ during desorption processing, and these heavy
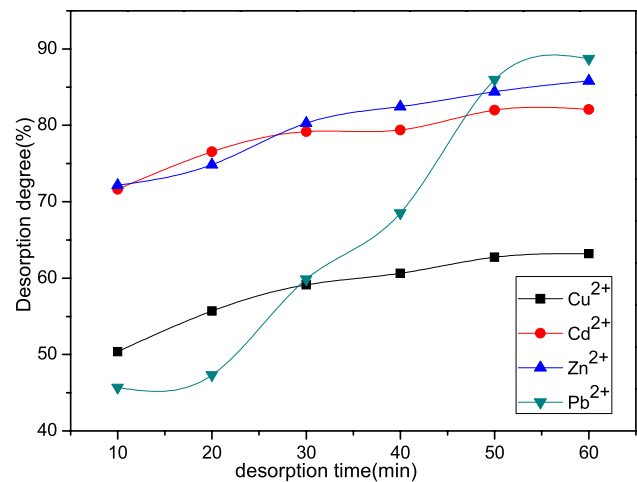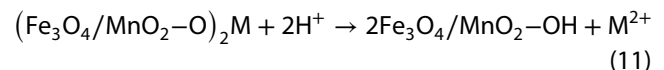

Fig. 11 The desorption ratio with time

metals ions were leased form structure. The desorption mechanism were expressed as:

$$\left(Fe_3O_4/MnO_2{-}O\right)_2 M + 2H^+ \rightarrow 2Fe_3O_4/MnO_2{-}OH + M^{2+} \tag{11}$$

The magnetic strengh of Fe_3O_4/MnO_2 composite carrying heavy metals was showed in Fig. 12. Results from the magnetic measurements show a drop in magnetic moment with increasing Mn concentration. Room temperature VSM measurements resulted in moments of 63.77 emu g^{-1} and 14.19 emu g^{-1} for Fe_3O_4 and Fe_3O_4/MnO_2 nano-composites carrying heavy metal ions. The process removes the Fe cations from the lattice and incomplete site replacement with the Mn^{2+} ions results in a disordered structure and significant loss of magnetic strength. Despite reduction in magnetic strength, there were enable magnetic manipulation and recovery of the Fe_3O_4/MnO_2 nano-composites sorbent. Fe_3O_4/MnO_2 nano-composites
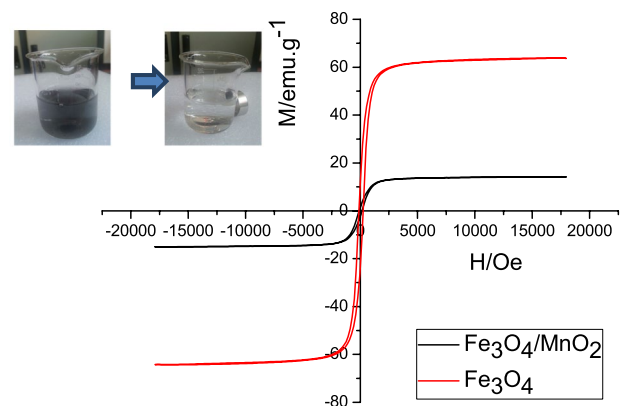
Fig. 12 Magnetic strength of Fe_3O_4/MnO_2 composite carrying heavy metals

were rapidly collected within seconds from suspension liquid by an external magnetic field. The result showed the Fe_3O_4/MnO_2 nano-composites were not only a kind of adsorbent which could remove the heavy metal ions in the water, but also could be collected with magnets. In addition, with gently shaking the separated adsorbent particles were easily re-dispersedto fairly stable suspension, which was essentially important for the convenient reuse of Fe_3O_4/MnO_2 nano-composites. In fact, the weak magnetic materials could be better dispersed in aqueous solution, which could provid more surface active sites and better water purification performance.

For the recycling experiments, Fe_3O_4/MnO_2 composites sample was initially contacted for 24 h in wastewater bearing heavy metals such as Cu^{2+}, Cd^{2+}, Zn^{2+} and Pb^{2+} (pH 6.5) with a sorbent dosage of 1 g L^{-1}. The sorbents of Fe_3O_4/MnO_2 composites carring heavy metals were colleted with a magnet and the heavy metals were stripped from the sorbent using a 1 h rinse in 0.1 M HCl. The unloaded sorbents were used to remove heavy metals from wastewater again and again.

The Fe_3O_4/MnO_2 composites had high potential to adsorption heavy metal ions after 5 times cycle removing Cu^{2+}, Cd^{2+}, Zn^{2+}, Pb^{2+} from wastewater. The cycles of adsorption and desorption of the Cu^{2+}, Cd^{2+}, Zn^{2+}, Pb^{2+} were shown in Fig. 13. The removal efficiency increased from 97.55 to 99.76% for Cd^{2+} sorption, in latter three tiems cycles the removal efficiency slightly floating up and down at 99.6%. The removal efficiency increased from 97.55 to 98.62% for Pb^{2+} sorption, at latter three times cycles, the removal efficiency was up to 98%. For Cu^{2+}, the removal efficiency decreased from 97.8 to 95.7% in the second cycle, but it increased again in the last three cycles, and it could be found thatthe efficiencyremained as high as

99.6% after five cycles. The increase of removal efficiency in the process of recycling might be due to the fact that the large bulks of adsorbent break into smallones, leading more active sites were exposed during the repeated cycles. The adsorption Zn^{2+} degree of Fe_3O_4/MnO_2 nano-composites was 85% after 5 times recycle.

The recycle utilization efficiency of Fe_3O_4/MnO_2 composites was showed in inside Fig. 13. The dosage was 1 g L^{-1}, with every inial heavy ion contents of 10 mg L^{-1}, and the temperature of 30 °C. The y-axis was split to allow for observation of the differences cycle in the remove of Cd^{2+} for each adsorption/desorption cycle. The arrow tip was added to enhance clarity of the Cd^{2+} adsorption and desorption steps of the cycles, respectively. Initial contact showed almost complete adsorption of Cd^{2+} (96.5%), followed by nearly complete stripping of the Cd^{2+} by the HCl wash step. The cycle was repeated with Cd^{2+} loading followed by nearly complete removal by the HCl wash step for five cycles with capture efficiencies of 96.5, 99, 98, 99 and 97% Cd for the subsequent cycles. The five times accumulation of Cu^{2+}, Cd^{2+}, Pb^{2+} remove from water by core–shell structure Fe_3O_4/MnO_2 was over 2375 mg g^{-1} respectively. The five times accumulation for Zn^{2+} was 2017.5 mg g^{-1}. The core–shell streucture Fe_3O_4/MnO_2 had the performance of adsorption–desorption and provided cost-effective, high efficiency, and magnetically manipulable sorbents which could be enable a range of remediation, recycling, and analytical solutions.

4 Conclusions

Magnetic Fe_3O_4/MnO_2 nano-composites demonstrated the ability to removel heavy metals from insustrial wastewater. The results showed that Fe_3O_4/MnO_2 Core–shell nano-composite was a friendly environments with higher affinity and capacity to removal heavy metals from water. The results showed in follow:

The heavy metal ions removal result showed that Fe_3O_4/MnO_2 nano-composites adsorption capacity of heavy metal ions on was high and the removal ratios of heavy metals were exceeded 99%. The equilibrium data analysis indicated that the Langmuir model was the most appropriate model to describe the adsorption of on the surface of Fe_3O_4/MnO_2 composites. The kinetics studies showed that the adsorption kinetics of heavy metal ions on the surface of the sorbent was significantly appropriate to pseudo-second-order model.

The adsorbed metal ions substituted the hydrogen atoms and formed new complex with oxygen in the homologous functional groups. The heavy metals substituted for H of Mn–O–H and formed the structure of Mn–O–Cu, Mn–O–Cd, Mn–O–Zn and Mn–O–Pb
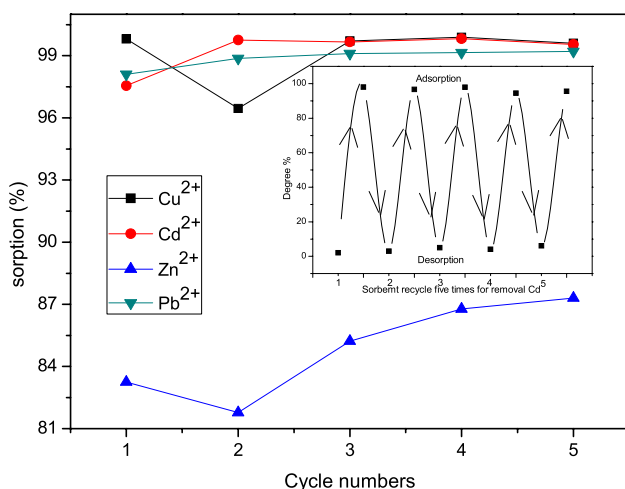

Fig. 13 Fe_3O_4/MnO_2 composites adsorption–desorption for five cycles

which meant the metals remove was the process of ion exchange. The adsorption of heavy metal ions on Fe_3O_4/MnO_2 nano-compositeswas dependent on pH and with the dose of sorbent. Recycle times of removal results suggest that magnetic Fe_3O_4/MnO_2 nano-composites could be removed heavy metal ions from wastewater effectively.

Compliance with ethical standards

Conflict of interest The authors declare that they have no conflicts of interest to this work.

References

1. Jaishankar M, Tseten T, Anbalagan N, Mathew BB, Beeregowda KN (2014) Toxicity, mechanism and health effects of some heavy metals. Interdiscip Toxicol 7:60–72
2. Sharma RK, Agrawal M, Marshall F (2007) Heavy metal contamination of soil and vegetables in suburban areas of Varanasi, India. Ecotoxicol Environ Saf 66:258–266
3. Barbosa F Jr (2017) Toxicology of metals and metalloids: promising issues for future studies in environmental health and toxicology. J Toxicol Environ Health Part A 80(3):137–144
4. Shih YJ et al (2013) Application of Fered-Fenton and chemical precipitation process for the treatment of electroless nickel plating wastewater. Sep Purif Technol 104:100–105
5. Maleki A, Hajizadeh Z, Sharifi V, Emdadi Z (2019) A green, porous and eco-friendly magnetic geopolymer adsorbent for heavy metals removal from aqueous solutions. J Clean Prod 215:1233–1245
6. Terbouche A, RamdaneTerbouche CA, Hauchard D, Djebbar S (2011) Evaluation of adsorption capacities of humic acids extracted from Algerian soil on polyaniline for application to remove pollutants such as Cd(II), Zn(II) and Ni(II) and characterization with cavity microelectrode. J Environ Sci 23(7):1095–1103
7. Azimi A, Azari A, Rezaazemi M, Ansarpour M (2017) Removal of heavy metals from industrial wastewaters: a review, Weiheim. Chem BioEng Rev 4:1–24
8. Badruddoza AZ, Shawon ZB, Tay WJ, Hidajat K, Uddin MS (2013) Fe_3O_4/cyclodextrin polymer nanocomposites for selective heavy metals removal from industrial wastewater. Carbohydr Polym 91(1):322–332
9. Javadian H, Ghorbani F, Tayebi H-A, Asl SH (2015) Study of the adsorption of Cd(II) from aqueous solution using zeolite-based geopolymer, synthesized from coal fly ash; kinetic, isotherm and thermodynamic studies. Arab J Chem 8:837–849
10. Choumane R, Peulon S (2019) Electrodeposited birnessite thin film: an efficient eco-friendly sorbent for removing heavy metals from water. Colloids Surf A 577:594–603
11. Dabrowski A, Hubicki Z, Podkoscielny P, Robens E (2004) Selective removal of the heavy metal ions from waters and industrial wastewaters by ion-exchange methode. Chemosphere 56:91–106
12. Xiao Q, Sun Y, Zhang J, Li Q (2015) Size-dependent of chromium(VI) adsorption on nano-Fe_2O_3 surface. Appl Surf Sci 356:18–23
13. Mustafa S, Waseem M, Naeem A, Shah KH (2010) Selective sorption of cadmium by mixed oxides of iron and silicon. Chem Eng J 157(1):18–24
14. Kara İ, Yilmazer D, Akar ST (2017) Metakaolin based geopolymer as an effective adsorbent for adsorption of zinc(II) and nickel(II) ions from aqueous solutions. Appl Clay Sci 139:54–63
15. Qiu R, Cheng F, Huang H (2018) Removal of Cd from aqueous solution using hydrothermally modified circulating fluidized bed fly ash resulting from coal gangue power plant. J Clean Prod 172:1918–1927
16. Koetlisi KA, Muchaonyerwa P (2019) Sorption of selected heavy metals with dierent relative concentrations in industrial effluent on biochar from human faecal products and pine-bark. Materials 12:1768
17. Han R, Zou W, Li H, Li Y, Shi J (2006) Copper(II) and lead(II) removal from aqueous solution in fixed-bed columns by manganese oxide coated zeolite. Hazard Mater 137(2):934–942
18. Obaid SS, Gaikwad DK, Sayyed MI, AL-Rashdi K, Pawar PP (2018) Heavy metal ions removal from waste water bythe natural zeolites. Mater Today Proc 5(9):17930–17934
19. Horst MF, Alvarez M, Lassalle VL (2016) Removal of heavy metals from wastewater using magnetic nanocomposites: analysis of the experimental conditions. Sep Sci Technol 51:550–563
20. Hua M et al (2012) Heavy metal removal from water/wastewater by nanosized metal oxides: a review. J Hazard Mater 211(15):317–331
21. Warner CL, Chouyyok W, Mackie KE, Neiner D, Saraf LV, Droubay TC, Warner MG, Addleman RS (2012) Manganese doping of magnetic iron oxide nanoparticles: tailoring surface reactivity for a regenerable heavy metal sorbent. Langmuir 28:3931–3937
22. Yan J, Khoo E, Sumboja A, Lee PS (2010) Facile coating of manganese oxide on tin oxide nanowires with high-performance capacitive behavior. ACS Nano 4(7):4247–4255
23. Islam MdA, Morton D, Johnson B, Mainali B, Angove MJ (2018) Manganese oxides and their application to metal ion and contaminant removal from wastewater. J Water Process Eng 26:264–280
24. Chaudhry SA et al (2016) Adsorptive removal of Pb(II) and Zn(II) from water onto manganese oxide-coated sand: isotherm, thermodynamic and kinetic studies, Egypt. J Basic Appl Sci 3(3):287–300
25. Liu Z et al (2018) An efficient adsorption of manganese oxides/activated carbon composite for lead (II) ions from aqueous solution. Arab J Sci Eng 43(5):2155–2165
26. Vasconcellos CM, Gonçalves MLA, Pereira MM, Carvalho NMF (2015) Iron doped manganese oxide octahedral molecular sieve as potential catalyst for SO_x removal at FCC. Appl Catal A 498:69–75
27. Langmuir I (1916) The constitution and fundamental properties of solids and liquids. Part I. Solids. J Am Chem Soc 38:2221–2295
28. Nuri OS, Irannajad M, Mehdilo A (2019) Reagent adsorption on modified mineral surfaces: isotherm, kinetic and thermodynamic aspects. J Mol Liq 291:111311
29. Li E, Liang H, Du Z, Li D, Cheng F (2016) Adsorption process of octadecylamine hydrochloride on KCl crystal surface in various salt saturated solutions: kinetics, isotherm model and thermodynamics properties. J Mol Liq 221:949–953
30. McCafferty E (2010) Relationship between the isoelectric point (pH_{pzc}) and the potential of zero charge (E_{pzc}) for passive metals. Electrochim Acta 55(5):1630–1637
31. Luo C, Tian Z, Yang B, Zhang L, Yan S (2013) Manganese dioxide/iron oxide/acid oxidized multi-walled carbon nanotube magnetic nanocomposite for enhanced hexavalent chromium removal. Chem Eng J 234(3):256–265

Publisher's Note Springer Nature remains neutral with regard to jurisdictional claims in published maps and institutional affiliations.